

# Development of Ketoprofen-p-Aminobenzoic Acid Co-Crystal: Formulation, Characterization, Optimization and Evaluation

**Meenakshi Bhatia**

Guru Jambheshwar University of Science and Technology

**Ashwani Kumar**

Guru Jambheshwar University of Science and Technology

**Vikas Kumar**

Guru Jambheshwar University of Science and Technology

**Sunita Devi** (✉ [sunitamechu1504@gmail.com](mailto:sunitamechu1504@gmail.com))

Guru Jambheshwar University of Science and Technology

---

## Research Article

**Keywords:** Ketoprofen, p-aminobenzoic acid, Co-crystal, Solubility enhancement, Solvent evaporation.

**Posted Date:** June 16th, 2021

**DOI:** <https://doi.org/10.21203/rs.3.rs-596789/v1>

**License:**  This work is licensed under a Creative Commons Attribution 4.0 International License.

[Read Full License](#)

---

1 **Development of Ketoprofen-p-aminobenzoic acid Co-crystal: Formulation,**  
2 **characterization, optimization and evaluation**

3 Meenakshi Bhatia <sup>1</sup>, Ashwani Kumar<sup>1</sup>, Vikas Kumar<sup>2</sup> and Sunita Devi <sup>1\*</sup>

4 <sup>1</sup> *Departmental of Pharmaceutical Sciences, Guru Jambheshwar University of Science and Technology,*  
5 *Hisar, 125001, India*

6 <sup>2</sup> *Departmental of Chemistry, Guru Jambheshwar University of Science and Technology, Hisar, 125001,*  
7 *India*

8

9

10

11

12

13

14

15

16

17

18

19

20 \*Corresponding author:

21 Sunita Devi,

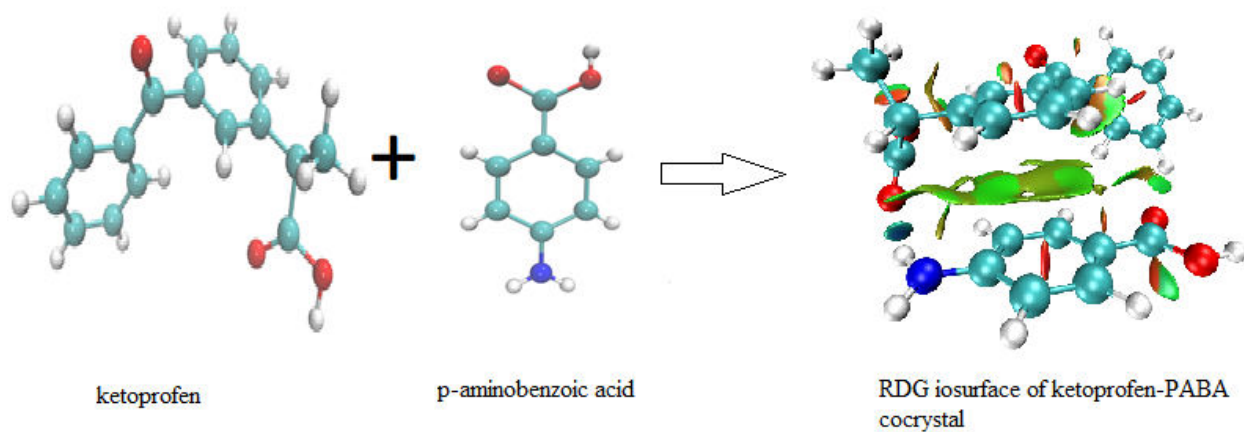
22 Drug Delivery Research laboratory, Department of Pharmaceutical Sciences,

23 Guru Jambheshwar University of Science and Technology, Hisar, 125001, India

24 e-mail: [sunitamechu1504@gmail.com](mailto:sunitamechu1504@gmail.com)

25

26 **Grapical abstract**



27

28

29

30

31

32

33

34

35

36

37

38

39

40

41

42

43

44 **ABSTRACT**

45 Co-crystal is a promising class of solids that may provide options for improved properties. In the  
46 present study, ketoprofen- *p*-aminobenzoic acid (KP-PABA) co-crystal were prepared to sought  
47 enhanced solubility and dissolution rate of drug. KP-PABA co-crystal were prepared by solvent  
48 evaporation technique employing central composite experimental design, selecting independent  
49 variables as concentration of drug and PABA whereas dependent variables were assumed to be  
50 solubility and % drug release. The optimized batch as suggested by the experimental design was  
51 characterized by FTIR, DSC, XRD, SEM and NMR studies and further, evaluated for *in-vitro*  
52 and *in-vivo* anti-inflammatory and analgesic activities. The solubility and % drug release of  
53 different batches of co-crystal was found to be between 34.20-60.11 µg/ml and 68.11-93.45%,  
54 respectively. Co-crystal containing ketoprofen and PABA in molar ratio (1:1) was found to be  
55 optimized formulation batch. Physical characterization by X-ray diffraction spectra and  
56 differential scanning calorimetric studies confirms the crystallinity of prepared co-crystal. The  
57 half maximal inhibitory concentration (IC<sub>50</sub>) values for *in-vitro* anti-inflammatory activity comes  
58 out to be 34.04 µM for ketoprofen and 4.373µM for optimized formulation, exhibiting almost 8-  
59 fold amplification indicating higher anti-inflammatory effect of optimized batch as compared to  
60 drug ketoprofen. The results of *in-vivo* anti-inflammatory activity carried out by rat paw edema  
61 method revealed that the optimized batch of co-crystal preparation provided a significant %  
62 inhibition in paw volume in contrast to standard drug in wistar rats. In this case, a crystalline  
63 molecular complex of drug Ketoprofen, that demonstrate poor aqueous solubility, with *p*-  
64 aminobenzoic acid was recognized that further set out an improvement in solubility and also in  
65 anti-inflammatory activity of the drug in wistar rats.

66 **KEY WORDS:** Ketoprofen. *p*-aminobenzoic acid. Co-crystal. Solubility enhancement. Solvent  
67 evaporation.

68

69

70

71

72

## 73 INTRODUCTION

74 Co-crystal are described as a multicomponent crystalline material possessing two or more  
75 molecules (i.e., drug and coformer) that are connected by noncovalent interactions in the same  
76 crystal lattice [1,2]. Co-crystal have the ability to improve the drug dissolution, bioavailability,  
77 hygroscopicity, solubility, processability and physical/chemical stability of the compound as  
78 compared to active pharmaceutical ingredient (API) [3, 4]. Co-crystallization is an advanced  
79 method to improve pharmaceutical solid dosage form. The preference of a method to produce co-  
80 crystal is crucial and depends on different factors for example thermal stability, alteration in  
81 solubility of coformers and API in particular solvents, tendency to form stable polymorphs or  
82 solvates and availability of a sufficient amount of the substance [5]. The selection of suitable  
83 coformer for co-crystallization is based on aqueous solubility of coformer, hydrogen bonding,  
84 non-covalent bonding, carbon chain length and molecular recognition. The difference between  
85 pKa value of API and coformer (i.e.,  $\Delta pK_a$ ) also depicts the co-crystal formation capability of a  
86 coformer with a given API [6, 7]. According to Berry and Steed, salt formation occurs when  
87  $\Delta pK_a$  value remains in close proximity to that of a base however co-crystal will be formed if this  
88 value exists close to acid [8]. The formation of co-crystal is formed if multiple H-bonds are  
89 formed [9, 10]. Co-crystal of various drugs with different coformers are listed as ketoconazole  
90 with *p*-amino benzoic acid and nicotinamide, telmisartan with chitosan, aceclofenac with  
91 chitosan, tadalafil with methylparaben, carbamazepine with nicotinamide, piroxicam with PEG  
92 4000, PVP K30, acetazolamide with theophylline and piperazine and 5-Fluorouracil with  
93 gentisic acid, 3,4-dihydroxybenzoic acid and 4-aminopyridine etc. that have been synthesized  
94 employing different techniques *viz.* solvent evaporation [11], solvent change approach [12, 13],  
95 solvent drop grinding [14], solution cooling crystallization, solvent evaporation, melting and  
96 cryomilling [15], slow crystallisation [16], liquid-assisted grinding and solvent evaporation [17],  
97 solvent-assisted grinding and solution crystallization [18].

98 Ketoprofen ( $C_{16}H_{14}O_3$ ) belongs to BCS-II, is a propionic acid derivative and can be taken orally  
99 to treat inflammatory diseases for instance rheumatoid arthritis, osteoarthritis, musculoskeletal  
100 disorders or postoperative pain etc. [19]. The anti-inflammatory property of ketoprofen is due to  
101 inhibition of enzyme cyclooxygenase-I and II, thus curtailing the formation of precursors of

102 prostaglandins and thromboxanes. Several methods of improving the solubility or dissolution  
103 rate of ketoprofen have been put forward like solid dispersion [20, 21], liquisolid [22],  
104 microemulsion-based gel [23], emulgels [24], nanoparticles [25-27], solid  
105 lipid nanoparticles (SLNs) [28], prodrug with pectin [29], micro and nanocomposite with PLGA  
106 [30] etc. Although the co-crystal of ketoprofen with conformer nicotinamide [31] are known. *P*-  
107 aminobenzoic acid (PABA) as a conformer proposed in this study is a member of the vitamin B  
108 complex and is generally recognized as safe (GRAS) [32]. The ketoprofen and PABA were  
109 selected on the basis of the pKa rule. Benzoic acid has pKa value of 4.21 whereas pKa value for  
110 ketoprofen is 3.88 and the value of  $\Delta pK_a$  ( $pK_{a_{acid}} - pK_{a_{base}}$ ) is -1.36 and correlate to Bhogala et  
111 al., at negative values of  $\Delta pK_a$ , co-crystal development is predictable [33].

112 In the present piece of research-work, easy and consistent technique of solvent evaporation was  
113 employed for composing the ketoprofen-PABA co-crystal seeking improved dissolution of drug.  
114 The preparation of co-crystal was accomplished as per central composite experimental design  
115 (CCD) by experimental design protocol selecting 2-factors at 3 levels (Design Expert software  
116 version 11.0). DSC, FT-IR, XRD, SEM and NMR studies were utilized to characterize the  
117 optimized formulation. The optimized formulation was further evaluated for both *in-vitro* and *in-*  
118 *vivo* activities.

## 119 **MATERIALS AND METHODS**

### 120 **Materials**

121 Ketoprofen (KP) was obtained from Infinity Laboratories Pvt. Ltd (Behra, India). *p*-amino  
122 benzoic acid (PABA) was supplied by Central Drug House (P) Ltd., New Delhi. Sodium  
123 chloride, acetic acid, carrageenan, ethanol, di-sodium hydrogen orthophosphate, potassium di-  
124 hydrogen orthophosphate was procured from Hi-Media lab. Pvt. Ltd. All other chemicals &  
125 reagents used in the study were of analytical grade and used as received.

### 126 **Methods**

#### 127 **Synthesis of Ketoprofen - *p*-amino benzoic acid (KP-PABA) co-crystal**

128 Ketoprofen - *p*-amino benzoic acid (KP-PABA) co-crystal was prepared by the solvent  
129 evaporation method as reported earlier [34]. Ketoprofen and PABA were used in  
130 stoichiometrically equal ratio and after carefully weighing were dissolved in 10mL of acetic acid

131 in a sealed flask and is kept under continuous stirring on a magnetic stirrer for 2 h while  
132 maintaining the temperature at 60 °C. The clear solution so formed was then filtered through  
133 5µm filter paper and allowed to evaporate slowly at room temperature under a fume hood.

### 134 **Experimental Design**

135 The preparation of co-crystal using ketoprofen and PABA was optimized using 2-factor, 3 level  
136 CCD. The concentration of ketoprofen (254.29-508.58 mg) ( $X_1$ ) and concentration of PABA  
137 (137.14-274.28 mg) ( $X_2$ ) were designated as formulation variables whereas the % drug release  
138 and solubility (µg/ml) were picked as response variables (Table I). Each independent variable  
139 was considered at three levels (i.e. -1, 0, and 1).

### 140 **Solubility studies**

141 Ketoprofen pure drug and each batch of KP-PABA co-crystal formulations containing  
142 ketoprofen equivalent to 10 mg was dispersed in 10 ml of distilled water, separately and are kept  
143 on continuous shaking for 48 h for equilibration at room temperature (25°C) to determine the  
144 solubility of ketoprofen. The obtained solution was filtered by 0.45µm millipore filter paper and  
145 the drug content was determined by taking absorbance at 260 nm using *uv-vis*  
146 spectrophotometer. The amount of drug was calculated using the calibration curve in water.

### 147 **Determination of drug content**

148 The different batches of KP-PABA co-crystal formulations containing drug equivalent to 5mg  
149 were dissolved separately in 25 ml of phosphate buffer (pH 7.4). The samples were filtered  
150 through 0.45µm milipore filters and after appropriate dilution the samples were analyzed by *uv-*  
151 *vis* spectrophotometer at 260nm [35].

152 Total Drug Content (TDC) was calculated by the following equation.

$$153 \text{ Total drug content (\%)} = \frac{\text{Weight of drug in cocrystal}}{\text{Weight of cocrystal}} \times 100 \quad (1)$$

### 154 ***In vitro* drug release profile**

155 *In vitro* dissolution studies were performed using USP type II dissolution apparatus. Dissolution  
156 studies of pure drug (Ketoprofen) and each batch of KP-PABA co-crystal formulation containing  
157 drug equivalent to 20 mg were conducted in 900ml phosphate buffer (pH 7.4) at 37±0.5°C with a

158 continuous stirring speed of 50 rpm. The powder was dispersed over the dissolution medium.  
159 Aliquots of sample (5ml) was withdrawn at different time intervals for 60 minutes and replaced  
160 with an equivalent amount of the dissolution medium to retain sink conditions during the  
161 experiment. Samples were filtered through 0.45µm milipore filters and the concentration of  
162 ketoprofen in the samples was determined by measuring the absorbance of the samples at a  
163 wavelength of 260 nm using the *uv-vis* spectrophotometer followed by determination of  
164 mechanism of release by fitting the release rate data in various release kinetic models.

## 165 **Characterization**

### 166 **Fourier Transform Infrared Spectroscopy (FT-IR)**

167 Ketoprofen, PABA and optimized batch of KP-PABA co-crystal formulation were exposed to  
168 FT-IR spectroscopy. FTIR spectroscopy was directed by a Perkin-Elmer, Spectrum, US  
169 spectrophotometer and the spectrum was documented in the wavelength region of 4000cm<sup>-1</sup> to  
170 400 cm<sup>-1</sup> using KBr pellet method. The method involves dispersing of sample in KBr and  
171 compressing into disc by applying a pressure of 50 kg/cm<sup>2</sup> in hydraulic press.

### 172 **Powder X-ray diffraction (PXRD)**

173 The ketoprofen, PABA, and optimized batch of KP-PABA co-crystal formulation powder  
174 samples were examined using an X-ray diffractometer (Miniflex 2, Rigaku, Japan) from 0° to 80°  
175 diffraction angle (2Θ). The Miller index (d<sub>hkl</sub>) signifies direction and plane in the crystal and is  
176 determined using Bragg's equation (equation 2).

$$177 \quad n\lambda=2d_{hkl}Sin\theta \quad (2)$$

178 Here λ and n denote the wavelength (1.5418Å) and order (n=1, first order), respectively; θ is the  
179 Bragg's angle.

### 180 **Differential scanning Calorimetry (DSC)**

181 Thermal behavior of ketoprofen, PABA and optimized batch of KP-PABA co-crystal  
182 formulation was studied using a DSC (Mettler Toledo, Switzerland), heated the samples at

183 temperatures within the range of 20-250°C with a scanning rate of 10°C/min in aluminum pans  
184 under nitrogen flow at a rate of 50 ml/min.

### 185 **Scanning electron microscopy (SEM)**

186 The surface morphology and shape of optimized batch of KP-PABA co-crystal formulation was  
187 examined using SEM (JSM-6100 scanning microscopy, Japan). The sample (optimized batch)  
188 after coated with gold was mounted on aluminium stub containing double adhesive carbon tape.  
189 The photographs were observed at acceleration voltage of 10 kV.

### 190 **Nuclear Magnetic Resonance (NMR) Spectroscopy**

191 The NMR spectra of ketoprofen, PABA and optimized batch of KP-PABA co-crystal  
192 formulation after dissolving in DMSO-d<sub>6</sub> were examined using Bruker Avance AV 400 NMR  
193 spectrometer (Bruker, Karlsruhe, Germany) to get solution <sup>13</sup>C NMR data at a temperature of  
194 293 K using Tetramethylsilane (TMS) as an internal standard [36]. Data was interpreted using  
195 Mnova program (Mestrelab Research, Santiago de Compostela, Spain).

### 196 **Stability studies**

197 The optimized batch of co-crystal was kept for the accelerated stability studies according to ICH  
198 guidelines (40 ± 2 °C and 75 ± 5% RH) for a period of 6 months in a stability chamber. The  
199 samples were placed in hermetically sealed vials containing rubber plugs and aluminum bung.  
200 The stored co-crystal were taken out after 6 months and evaluated for the drug content  
201 (according to the method described in earlier section of drug content, *n*=3) and for any physical  
202 changes [13].

### 203 **Biological evaluation of KP-PABA co-crystal**

#### 204 ***In-vitro* anti-inflammatory activity**

205 Egg albumin denaturation method was employed to evaluate *in-vitro* anti-inflammatory activity  
206 of drug ketoprofen and optimized batch of KP-PABA co-crystal [37]. The mixture contained of  
207 pure fresh hen's egg albumin (0.2ml), Phosphate buffer saline, pH 7.4 (2.8 ml)) and 2ml of  
208 different concentrations of KP-PABA co-crystal formulation (containing ketoprofen equivalent  
209 to 10 mg) (125, 250, 500, 750 & 1000 µg/ml in Dimethyl sulfoxide as solvent). After incubation  
210 (Caltan, NSW, India) for 15 min at a temp of 37±2 °C, the temperature of mixture was raised to

211 70°C. After cooling at room temperature, the absorbance measured at  $\lambda_{\max}$  of 260nm. Similar  
212 procedure is followed for the model drug ketoprofen containing same concentrations as for the  
213 formulation, as a reference or control [38].

214 The % inhibition of protein denaturation was calculated as per equation 3

$$215 \quad \% \text{ Inhibition} = \frac{\text{Abs.of control} - \text{Abs. of sample}}{\text{Abs.of control}} \times 100 \quad (3)$$

216 The half maximal inhibitory concentration (IC<sub>50</sub>) values of ketoprofen and optimized formulation  
217 was measured by nonlinear regression analysis using Graph Pad Prism 5.0 for Windows.

### 218 ***In-vivo* carrageenan-induced anti-inflammatory activity**

219 The protocol with registration no. CPCSEA Reg. no-IAEC/2020/10-18 was approved for animal  
220 study by the Animal Ethical Committee, Guru Jambheshwar University of Science and  
221 Technology, Hisar, India. Wistar rats (180-210 g) of either sex were divided into three groups  
222 comprising of six animals each. Group I (Control treated) with carrageenan was kept as control,  
223 Group II (standard Drug) was treated with drug-ketoprofen (10 mg/kg) and Group III (Test  
224 compound) was treated with KP-PABA co-crystal (equivalent to ketoprofen 10 mg/kg) body  
225 weight administrated orally. 0.1 ml of 1% suspension of carrageenan in normal saline, was  
226 administered as subplantar injection in the left hind paw of albino wistar rats, after 1 h after of  
227 oral administration of the test materials. The paw volume was measured using vernier caliper at  
228 1, 2, 3, 4, 5 and 6 h after the carrageenan injection [39, 40]. The % inhibition in paw volume was  
229 calculated by using equation 4,

$$230 \quad \% \text{ inhibition} = \frac{V_c - V_t}{V_c} \times 100 \quad (4)$$

231 Where  $V_c$  and  $V_t$  is the inflammatory increase in paw volume control group and the  
232 inflammatory increase in paw volume in test group respectively [41].

### 233 **Analgesic activity (Tail flick method)**

234 Analgesic activity was measured by tail flick method using a radiant type analgesiometer. In tail  
235 flick method pain was produced by placing the tip of the tail on the heat source. Mice (25-30g)  
236 of either sex were divided into three groups (test, standard and control) containing six animals in  
237 each group. The tail flick reaction time for each animal was recorded six times before  
238 administering the drug and the mean was used as predrug reaction time. A dose of the standard  
239 drug (Ketoprofen) and test compound (optimized batch of KP-PABA co-crystal) containing

240 ketoprofen equivalent to 5 mg/kg of body weight in 0.9% w/v sterile saline was administered to  
 241 animals. The test and standard group received drug orally while the control group was catered  
 242 with vehicle only. After administration of the drug, the tail flick reaction time was measured at  
 243 different time interval as 0, 1, 2, 3, 4 and 5 h [42].

244 % Analgesic activity (PAA) was calculated by using the equation 5

$$245 \quad PAA = (T_2 - T_1)/T_1 * 100 \quad (5)$$

246 Where, T<sub>1</sub> and T<sub>2</sub> are reaction time in seconds before and after treatment with drug, respectively.  
 247 Data was analyzed by one-way ANOVA method and further followed by Tukey's post-hoc test,  
 248 statistically and is denoted as P value.

## 249 RESULTS

250 The preparation of co-crystal using ketoprofen and PABA was optimized using 2-factor, 3 level  
 251 CCD. The concentration of ketoprofen (X<sub>1</sub>) and concentration of PABA (X<sub>2</sub>) were designated as  
 252 formulation variables whereas the % drug release and solubility (µg/ml) were specified as  
 253 response variables Formulation parameters and responses for experimental design for different  
 254 batches of KP-PABA co-crystal as exhibited in Table 1. The TDC of different batches of KP-  
 255 PABA co-crystal was observed between 97.01 to 98.92 %. No physical changes were observed  
 256 during stability studies and even after six months.

### 257 Solubility studies

258 The outcome of solubility (Y<sub>1</sub>) and *in-vitro* drug release profile (Y<sub>2</sub>) of the KP-PABA co-crystal,  
 259 formulated according to the experimental design expert protocol is exhibited in Table I. The  
 260 responses generated were fitted into numerous polynomial models.

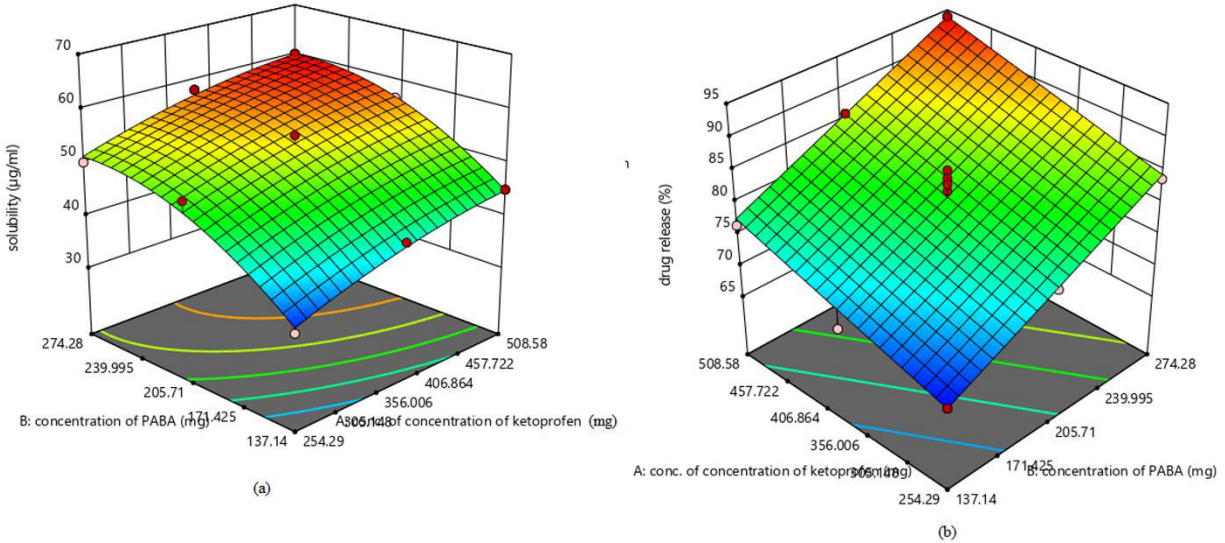
261 Table I. Formulation parameters and responses for experimental design.

Batch	Conc. Of Ketoprofen (mg) (X <sub>1</sub> )	Conc. Of PABA (mg) (X <sub>2</sub> )	Solubility (µg/ml) (Y <sub>1</sub> )	% <i>In-vitro</i> drug release in 60 min. (Y <sub>2</sub> )	Total drug content (%)
1	508.58	137.14	45.02±0.18	79.47±0.33	97.78±0.13
2	381.43	205.71	53.42±0.3	85.12±0.36	98.42±0.04

3	381.43	274.28	58.14±0.2	85.69±0.22	97.12±0.08
4	381.43	205.71	53.12±0.21	82.94±0.41	97.94±0.06
5	381.43	205.71	55.19±0.19	79.80±0.34	97.91±0.08
6	381.43	137.14	42.32±0.22	69.74±0.8	97.70±0.03
7	508.58	274.28	60.11±0.26	93.45±0.15	98.92±0.02
8	381.43	205.71	52.23±0.27	83.87±0.09	98.06±0.04
9	508.58	205.71	56.63±0.33	85.86±0.096	98.14±0.06
10	254.29	205.71	49.71±0.8	75.90±0.05	97.91±0.03
11	254.29	137.14	34.20±0.9	68.11±0.73	97.78±0.01
12	254.29	274.28	50.16±0.6	83.77±0.72	97.01±0.03
13	381.43	205.71	52.58±0.13	88.11±0.77	98.90±0.06
Ketoprofen			14.94±0.3	22.79±0.56	

262 All values are expressed as mean ± S.D., n=3.

263 The responses, solubility ( $Y_1$ ) and *in-vitro* drug release ( $Y_2$ ) were fitted best into the quadratic  
264 response surface model with none transformation of the data. In different batches of KP-PABA  
265 co-crystal solubility values range from 34.20 - 60.11 µg/ml and % *in-vitro* drug release range for  
266 68.11 to 93.45%. This upheave in solubility and thus dissolution may be due to formation of  
267 soluble complex between ketoprofen and PABA. The solubility of KP-PABA co-crystal (60.11  
268 µg/ml) was higher than that of the ketoprofen (14.94 µg/ml). The reason for this furtherance in  
269 solubility is the intermolecular hydrogen bonding between the ketoprofen and PABA and it is  
270 surmised that this linkage may result in hydration of co-crystal and thereby, high solubility of the  
271 drug is observed from co-crystal.



272

273 Figure 1. (a, b) Response surface plots displaying effect of concentration of ketoprofen (KP) &  
 274 PABA on solubility ( $Y_1$ ) and *in-vitro* drug release ( $Y_2$ ).

275 The polynomial models for the responses solubility ( $Y_1$ ) and *in-vitro* drug release ( $Y_2$ ) can also  
 276 be expressed by the equation (6) and (7), respectively. The synergistic and antagonist effect is  
 277 explained by the positive and negative coefficient value for specific independent variables in the  
 278 polynomial equation (6) and (7), respectively. The equations generated revealed that both factors  
 279 independently exerted a significant effect on the solubility and *in-vitro* drug release. The  
 280 response surface plot [Figure 1 (a, b)] revealed that solubility and *in-vitro* drug release vary in  
 281 curvilinear fashion with an increase in the amount of each factor. However, the effect of the  
 282 concentration of PABA ( $X_2$ ) seems to be more pronounced as compared with that of  
 283 concentration of ketoprofen ( $X_1$ ).

284  $Y_1 = 53.68 + 4.61X_1 + 7.81X_2 - 0.275X_1X_2 - 1.45X_1^2 - 4.39X_2^2$  (6)

285  $Y_2 = 42.218 + 0.037X_1 + 0.119X_2 - 0.317X_1X_2 - 3.51X_1^2 - 3.31X_2^2$  (7)

286 The denouement of ANOVA test on the response surface quadratic model are summarized in  
 287 Table II demonstrated that model was found significant with lack of fit as non-significant. A  
 288 good correlation among experimental and predicted responses was specified with a good value of  
 289  $R^2$  ( $>0.9$ ). The adequate precision measuring signal to noise ratio (greater than 4) is desirable. In  
 290 this design, the ratio of 25.49 (solubility) and 23.05 (drug release) illustrated an adequate signal  
 291 that let the model to navigate design space. Figure 1 (a&b) display the combined effect of

292 concentration of ketoprofen & PABA on solubility and drug release. It can be interpreted from  
 293 the plots that independent and dependent variables exists in a curvilinear correspondence. It is  
 294 also inferred from the plot that higher level of ketoprofen & PABA results in increase in  
 295 solubility of formulation.

296 Table II. Model summary statistics

Model						Lack of Fit	
Response factors (Y)	F-value	Prob.>F	R <sup>2</sup>	Adequate Precision	C.V (%)	F-value	Prob.>F
Y <sub>1</sub>	20.58	<0.0001	0.975	25.49	2.81	2.31	0.218
Y <sub>2</sub>	49.19	<0.0001	0.907	23.05	2.88	1.56	0.34

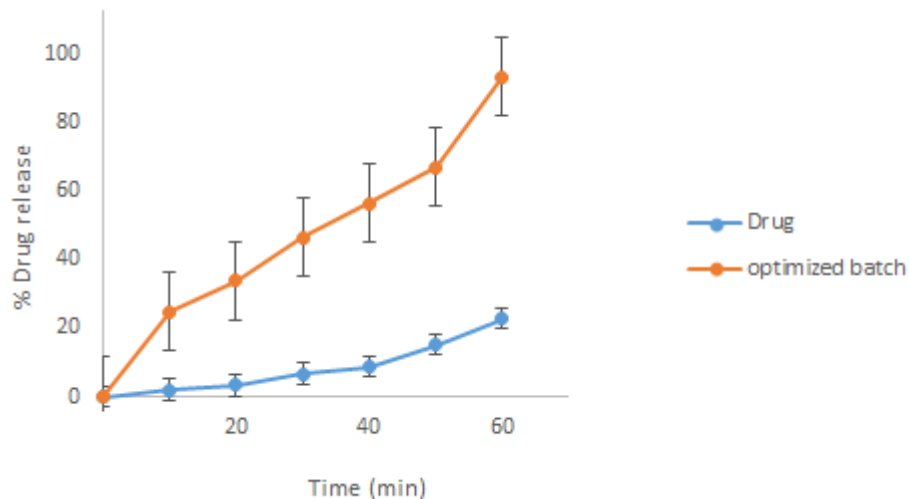
297

### 298 Optimization

299 The optimization equation 6 and 7, relating the response and independent factors, was fabricated  
 300 based on a quadratic model. To the responses *i.e.* solubility and *in-vitro* drug release the  
 301 desirability function was applied with constraints to obtain the higher magnitude of both. In this  
 302 manner the formulation, containing PABA (274.28 mg) as coformer and drug (508.58 mg) with  
 303 addition of acetic acid (2%) solution at 60°C, established the maximum desirability, was  
 304 organized and evaluated.

305 The optimization of independent variables was done with constraints of maximum solubility and  
 306 maximum % release. The different set of solutions are provided by the optimization tool in  
 307 design expert software. The parameters suggested by the design were concentration of  
 308 ketoprofen (508.58 mg) & concentration of PABA (274.28 mg) that provide co-crystal with  
 309 solubility of 60 µg/ml (predicted value 60.051 µg/ml) and % release 93.45% (predicted value  
 310 93.94%). The closer concordance between observed and predicted values discerned high  
 311 predictive ability of the model. Figure 2 displays the *in vitro* release profile of ketoprofen as pure  
 312 drug and the optimized batch of formulation.

313



314  
 315 Figure 2. *In-vitro* release profile of pure drug (Ketoprofen) and KP-PABA co-crystal (optimized  
 316 batch).

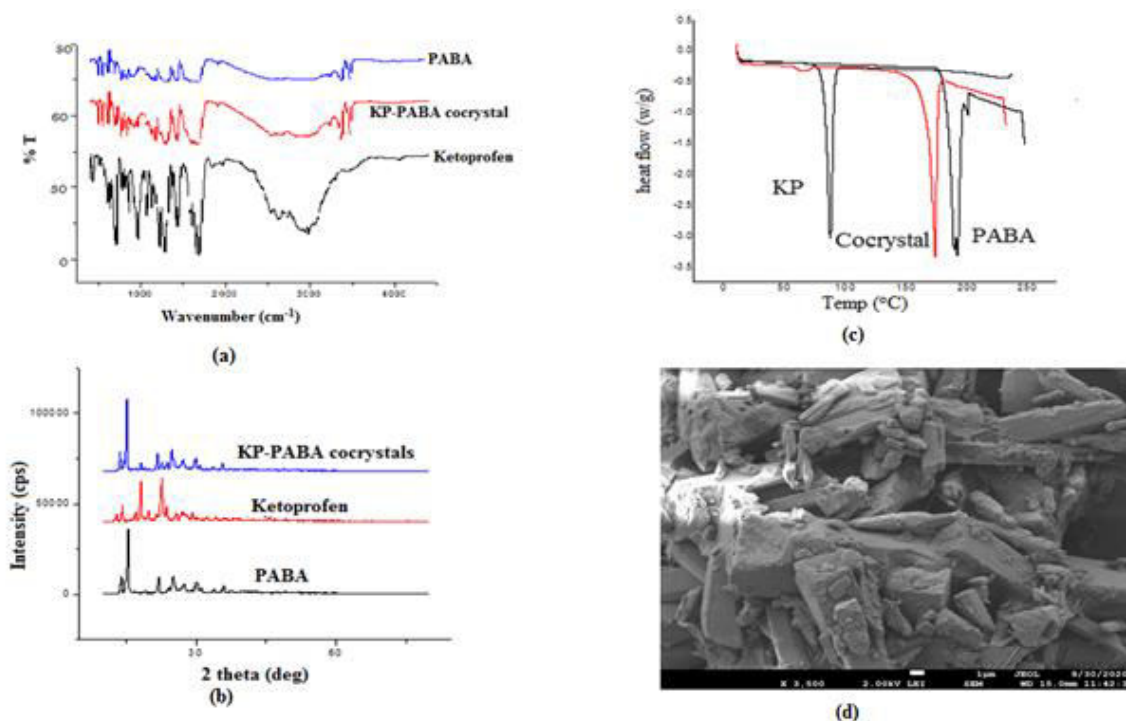
317 The release profile of co-crystal is compared with equivalent concentration of pure drug solution  
 318 to study release rate kinetics. The release of ketoprofen from co-crystal formulation and drug  
 319 solution was put into various kinetic models to estimate the kinetics and mechanism of release  
 320 (Table III). The release rate data for the formulation was found to be fitted best into Zero order  
 321 model of release kinetics ( $R^2 = 0.951$ ). Further, the value of 'n'  $> 1.0$  ( $n=1.4$ ) the release exponent  
 322 of Korsmeyer -Peppas equation indicated that the release of ketoprofen from co-crystal occurs  
 323 by super-case-2 transport *i.e.* the release occurred by relaxation or erosion of polymer after  
 324 swelling in biological fluid.

325 Table III. Modeling and release kinetics of ketoprofen from co-crystal.

Formulation	Zero order	First order	Higuchi	KorsmeyerPeppas	
	$R^2$	$R^2$	$R^2$	$R^2$	n
KP solution	0.915	0.850	0.949	0.808	1.48
Co-crystal	0.921	0.813	0.932	0.913	1.52

326  
 327 **FTIR Spectroscopy**  
 328 FTIR is an analytical method used to study the changes in the position caused by the vibration  
 329 modes of the functional groups. The FTIR spectra revealed the shift in characteristic peaks of

330 drug and coformer due to co-crystal formation involving H bonding between the corresponding  
331 functional groups. The spectra of ketoprofen figure 3 (a) showed characteristic absorption band  
332 at  $2979.27\text{ cm}^{-1}$  due to  $-\text{CH}$  stretching. The peak appearing at  $1697.76\text{ cm}^{-1}$  can be ascribed to -  
333  $\text{C}=\text{O}$  stretching of acid while peak appearing at  $1655.77\text{ cm}^{-1}$  is due to  $-\text{C}=\text{O}$  stretching of  
334 ketone. The absorption bands at  $1598.67\text{ cm}^{-1}$  ( $-\text{C}=\text{C}=\text{ stretching}$ ),  $1442.21\text{ cm}^{-1}$  ( $-\text{C}=\text{O}$   
335 stretching of aromatic ring),  $1420.59\text{ cm}^{-1}$  ( $-\text{C}-\text{H}$  deformation of  $\text{CH}_3$  asymmetrical) and  $1370.04$   
336  $\text{cm}^{-1}$  ( $-\text{C}-\text{H}$  deformation of  $\text{CH}_3$  symmetrical) also appeared. The spectra of PABA presented the  
337 characteristic absorption band of  $-\text{NH}$  stretch appearing at  $3461.24\text{ cm}^{-1}$ , peak at  $3362.37\text{ cm}^{-1}$  is  
338 due to  $-\text{OH}$  stretch, peak at  $1681.89$  is attributed to  $-\text{C}=\text{C}$  aromatic stretching while peak at  
339  $1422\text{cm}^{-1}$  may be ascribed to  $-\text{C}-\text{C}$  aromatic stretching. In FTIR spectra of KP-PABA co-crystal  
340 the peak due to  $-\text{C}=\text{O}$  stretching of  $-\text{COOH}$  group of ketoprofen shifted from  $1697.76\text{ cm}^{-1}$  to  
341  $1664.16\text{ cm}^{-1}$ . There was shift in  $-\text{NH}$  stretch from  $3362.37\text{ cm}^{-1}$  (PABA) to  $3360.95\text{ cm}^{-1}$  (KP-  
342 PABA co-crystal). These observations suggested formation of hydrogen bond between amino  
343 group of PABA and  $-\text{COOH}$  group of ketoprofen in KP-PABA co-crystal.



344  
345 Figure 3. (a) FTIR, (b) XRD, (c) DSC spectra of ketoprofen, PABA and optimized batch of KP-  
346 PABA co-crystal, (d) SEM image of optimized batch of KP-PABA co-crystal.

347

### 348 **Powder X-ray diffraction (PXRD)**

349 The X-ray diffraction spectra of ketoprofen, PABA and optimized batch of KP-PABA co-crystal  
350 is illustrated in figure 3 (b). In diffraction spectra of ketoprofen the peaks (and Miller indices)  
351 appeared at  $2\theta$  of 12.74 (100), 18.52 (200), 22.85 (211), 24.00 (221), 26.32 (222), 28.920 (300)  
352 whereas, in XRD spectra of PABA the peaks (and Miller indices) appeared 15.33(121), 22.67  
353 (211), 24.88 (221), 27.18 (222) and 30.65 (310) that manifested crystalline structure of  
354 ketoprofen and PABA respectively. The major diffraction peaks at  $2\theta$ , 13.32 (100), 15.90 (121),  
355 18.8 (200), 21.69 (210), 25.45 (221) and 27.19 (222) were also observed in PXRD spectra of co-  
356 crystal that portrayed crystalline nature of formulation this indicating that resultant product is  
357 also crystalline in nature [43]. Moreover, some characteristic peaks of ketoprofen at 12.74,  
358 22.85, and 28.92 disappeared while some peaks at 24.00 and 26.32 shifted to 25.45 and 27.19,  
359 respectively. Besides this, few peaks of PABA at 22.67 and 30.65 disappeared and few peaks at  
360 15.33, 24.88, and 27.18 shifted to 15.90, 25.45, and 27.19, respectively. These changes in the  
361 PXRD data of respective co-crystal from ketoprofen and coformer are suggestive of the  
362 formation of new forms.

363

### 364 **Differential scanning calorimetry (DSC)**

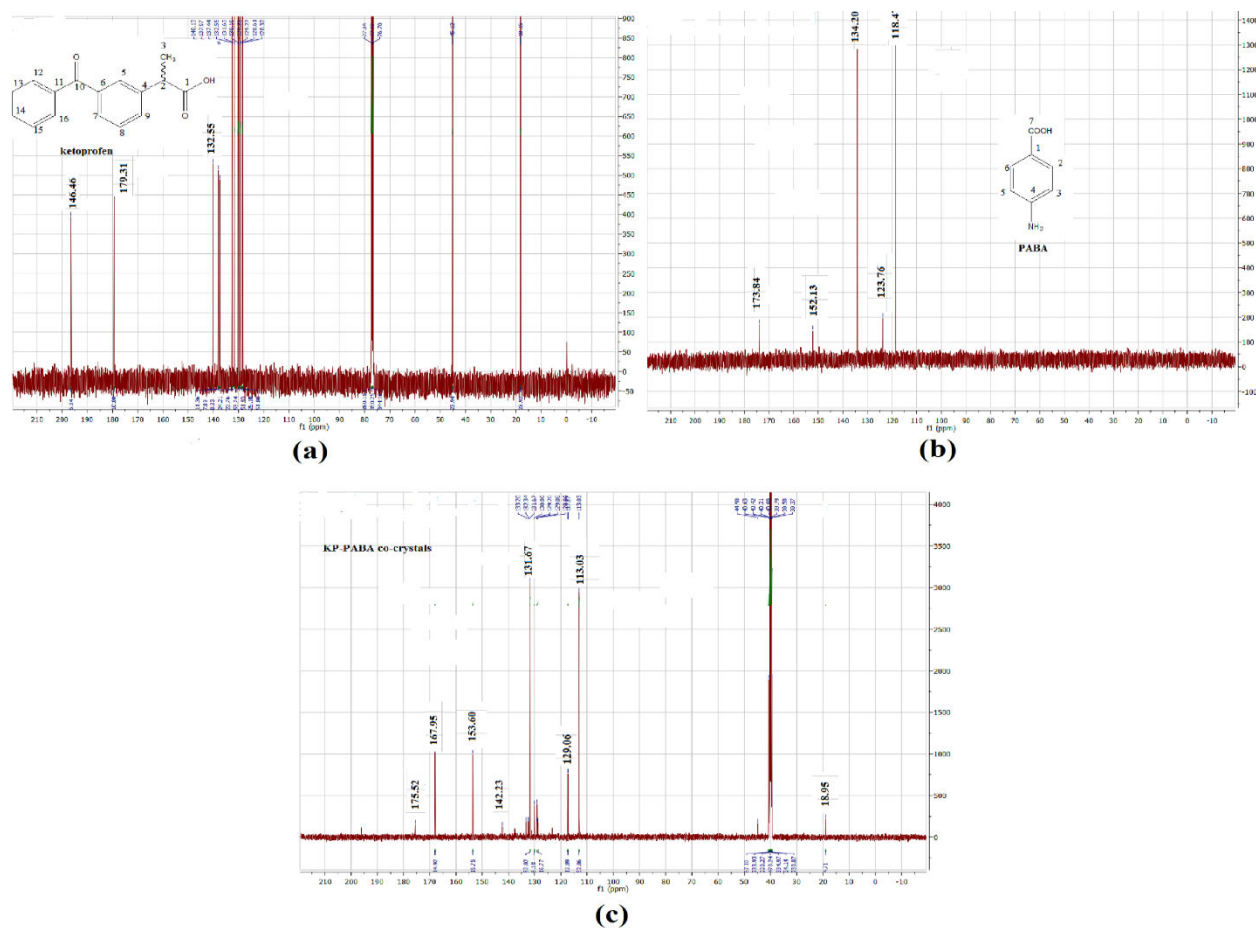
365 DSC thermogram (Figure 3 (c)) of ketoprofen displayed a sharp single peak at 94.5°C that  
366 corresponds to its melting point. The peak at 187.8°C attributed to melting point of PABA.  
367 However, in the DSC curve of co-crystal a single endothermic peak appearing at 180°C  
368 suggested the presence of a new phase (co-crystal) different from the constitutional components.  
369 The modification in the melting point is due to the alteration in the crystal lattice of the drug in  
370 the presence of coformer, indicating that certain modification has occurred.

### 371 **Scanning electron microscopy (SEM)**

372 The SEM image of the co-crystal formulation was depicted in figure 3 (d). The co-crystal  
373 showed good crystalline characteristics. This crystalline characteristic of co-crystal was  
374 reinforced by the XRD data, as discussed earlier. The pores over the surface of the co-crystal  
375 may brace the imbibition of the solvent/biological fluids, consequently, increasing the solubility  
376 and bioavailability of ketoprofen as anticipated.

377 **NMR Spectroscopy**

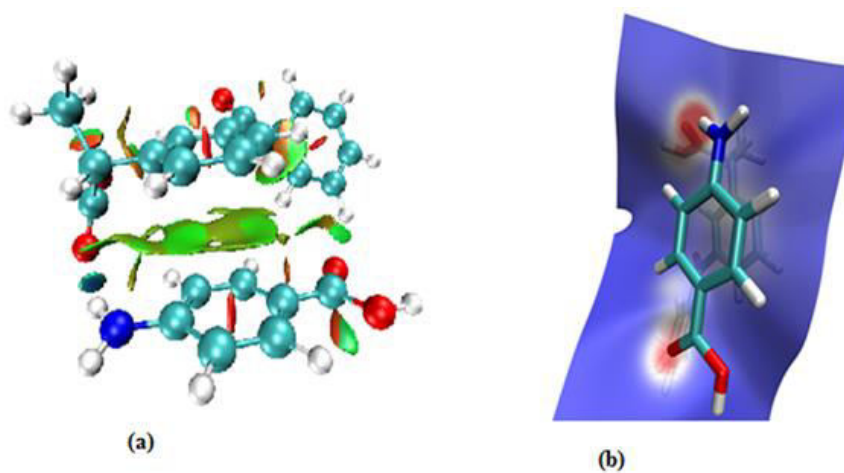
378 Nuclear magnetic resonance spectroscopy is used to characterize the co-crystal by studying the  
379 chemical environment of their nuclei and hydrogen bonding and it also offers valuable  
380 information regarding interactions. In the NMR spectra of KP-PABA co-crystal, the carbonyl  
381 carbon of ketoprofen corresponding to 196.46 ppm and 140.13 ppm has shifted to 196.12 ppm  
382 and 142.23 ppm, respectively. A deviation in the carbonyl carbon of carboxylic group in PABA  
383 shifted from 173.84 ppm and 152.13 ppm to 175.52 ppm and 153.60 ppm, respectively (Figure  
384 4). This suggests an interaction between amino group of PABA and –COOH group of ketoprofen  
385 in KP-PABA co-crystal.



390 **Non-covalent interactions (NCI) analysis**

391 Co-crystal involve no covalent modification of its constituents and different chemical  
392 constituents interact through non covalent interactions [44]. In order to identify the type of  
393 interactions that may be present in the cocrystal of ketoprofen and PABA, the NCI analysis was  
394 carried out. The chemical structures of ketoprofen and PABA were retrieved from pubchem  
395 database [<https://pubchem.ncbi.nlm.nih.gov>]. The two structures were combined and the system  
396 was minimized with molecular mechanics force field. This minimized system was further  
397 minimized using new and more accurate PM7 method by taking value of  $g_{norm}$  as 0.001 in  
398 MOPAC [45]. Different properties of the final minimized cocrystal were calculated by DFT  
399 using 6-31G\* basis set in B3LYP method of Firefly [46]. The interactions were determined using  
400 Multiwfn [47] and VMD [48].

401 Reduced density gradient (RDG) calculations show that one hydrogen bond is formed between  
402 carbonyl oxygen of the ketoprofen and hydrogen atom of amino group of PABA. Aromatic rings  
403 of both the molecules stacked against each other through pi-pi stacking interactions. Carbonyl  
404 oxygen atom of PABA made weak interactions with hydrogen atoms of terminal phenyl ring of  
405 ketoprofen. These interactions are shown in figure 5 (a) below:



406  
407 Figure 5. (a) RDG isosurface of ketoprofen-PABA cocrystal. Blue color indicates hydrogen bond  
408 and green and brown colors indicate weak Van der Waals interactions, (b) Hirshfeld surface  
409 mapped by electron density with promolecular approximation of ketoprofen-PABA co-crystal.

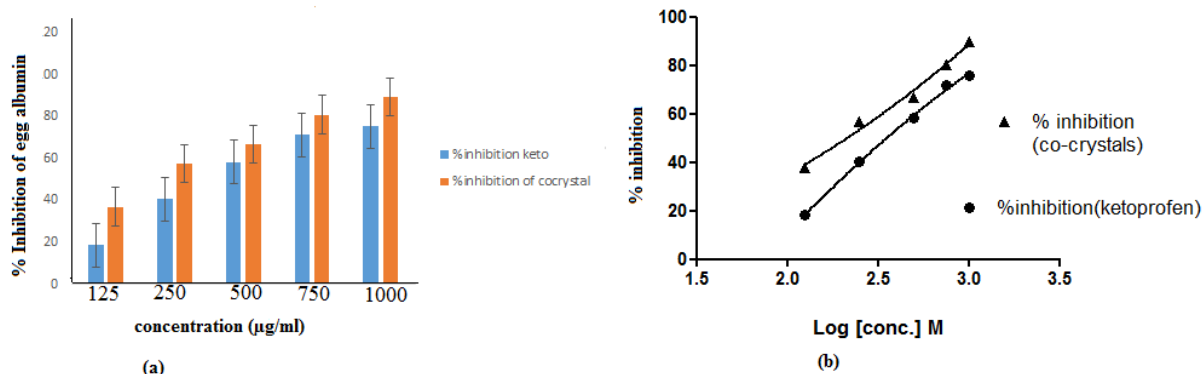
410

411 Further, Hirshfeld surface mapped by electron density with promolecular approximation analysis  
412 was also performed to study the hydrogen bond and Van der waals interactions. Figure 5 (b)  
413 shown here clearly indicate the region of high electron density in red color between PABA  
414 amino and ketoprofen carbonyl groups. Another one is present between PABA carbonyl and  
415 terminal phenyl protons of ketoprofen whereas white region between two aromatic rings depicts  
416 lesser electron density means weaker interactions blue color indicates electron free region.

## 417 **Biological evaluation of KP-PABA co-crystal**

### 418 ***In-vitro* anti-inflammatory activity**

419 The compared plot of % inhibition of protein denaturation at different concentration of optimized  
420 formulation and pure drug is shown in figure 6 (a). The plot displayed that as the concentration  
421 of drug is increased, the % inhibition is also got increased whereas the effect is more prominent  
422 at lower concentration range of drug. Nonlinear regression analysis was used to calculate the half  
423 maximal inhibitory concentration ( $IC_{50}$ ) values of ketoprofen and optimized formulation. The  
424  $IC_{50}$  values were  $34.04 \mu M$  for ketoprofen and  $4.373 \mu M$  for optimized formulation [Figure 6  
425 (b)], there is almost 8 fold improvement in  $IC_{50}$  value. Hence, it is concluded that co-crystal  
426 formulation is more active in producing anti-inflammatory response than the drug ketoprofen.



427  
428 Figure 6. (a) Percent inhibition of ketoprofen and optimized formulation, (b)  $IC_{50}$  values  
429 calculated using GraphPad Prism 5.0 for Windows.

### 430 ***In-vivo* anti-inflammatory activity**

431 Carrageenan induced rat paw edema method was appertained to compare oral efficacy of  
432 ketoprofen and optimized batch of KP-PABA co-crystal formulation. The improvement in

433 activity of ketoprofen and co-crystal formulation was comparatively assessed by the increase in  
 434 paw volume of control groups. The paw edema volume estimates (before and after drug  
 435 administration) and % inhibition of edema at different time interval was persuaded and displayed  
 436 in Table IV. The co-crystal and ketoprofen unveiled inhibition of paw edema as  $66.14 \pm 0.04\%$   
 437 and  $58.16 \pm 0.03\%$  at the end of 6 h, respectively thus demonstrating quick onset of action by co-  
 438 crystal in contrast with the pure drug ketoprofen.

439 Statical Analysis:- Data was compared by ANOVA followed by Tukey's test. The p value is  
 440  $<0.0005$  is considered as significant.

441 Table IV. Effect of ketoprofen and ketoprofen-PABA formulation on the paw edema induced by  
 442 carrageenan in Wistar rats.

Time (min)	Paw volume (mm)			Inibition (%)	
	Control	Pure drug	Co-crystal	Pure drug	Co-crystal
60	4.22±0.01	4.06±0.02*	4.01±0.01*	3.73±0.03	4.77±0.05 <sup>#</sup>
120	4.55±0.12	3.83±0.08*	3.71±0.14*	15.78±0.01	18.48±0.04 <sup>#</sup>
180	4.90±0.101	3.44±0.04*	3.17±0.07*	30.61±0.03	35.45±0.22 <sup>#</sup>
240	5.37±0.189	3.21±0.03*	3.02±0.03*	40.29±0.10	43.78±0.04 <sup>#</sup>
300	6.02±0.16	3.048±0.042*	2.863±0.61*	49.31±0.18	59.64±0.17 <sup>#</sup>
360	6.44±0.03	2.671±0.01*	2.138±0.03*	58.16±0.03	66.14±0.04 <sup>#</sup>

443 All values are expressed as mean ± S.D., n=6; \*Significant ( $p < 0.05$ ) compared to control; <sup>#</sup>Significant ( $p < 0.05$ ) compared  
 444 to pure drug (ketoprofen).

#### 445 Analgesic activity

446 The results of the % analgesic activity (PAA) of test, reference and control group are shown in  
 447 Table 5. The PAA (equation 5) was comparatively evaluated for KP-PABA co-crystal and pure  
 448 drug based on its potential to suppress pain. KP-PABA co-crystal showed significant effect in  
 449 enhancing the pain thershold to a certain extent when compared to that of drug (ketoprofen),  
 450 thus, stipulating that an improvement in solubility further tweaked the pharmacological response.

451

452 Table 5. % Analgesic effect of ketoprofen and KP-PABA by tail flick method in mice.

Treatment	PAA					
	0h	1h	2h	3h	4h	5h
Standard (ketoprofen)	0.03±0.020	31.30±0.71*	35.18±0.12*	42.36±0.17*	50.93±0.14*	71.96±0.17
Test (KP-PABA co-crystal)	0.02±0.011	35.51±0.15*	48.63±0.61*	55.84±0.14#	67.82±0.16#	78.92±0.32
Control (vehicle)	0.01±0.012	0.91±0.19	1.32±0.02	0.83±0.10	1.1±0.20	0.021±0.03

453 All values are expressed as mean ± S.D., n=6. \*Significant (p<0.05) compared to control. #Significant (p<0.05) compared to  
 454 pure drug (ketoprofen).

## 455 CONCLUSION

456 Ketoprofen-p-aminobenzoic acid co-crystals were prepared by solvent evaporation technique  
 457 employing central composite experimental design. The optimized batch containing ketoprofen  
 458 and PABA in molar ratio (1:1) after characterization by FT-IR, XRD, DSC, SEM and NMR  
 459 studies was further evaluated for *in-vitro* and *in-vivo* anti-inflammatory and analgesic activities.  
 460 The solubility and % drug release of different batches of co-crystal was found to be between  
 461 34.20-60.11 µg/ml and 68.11-93.45%, respectively. The results of *in-vivo* anti-inflammatory  
 462 activity by rat paw edema method provided a significant % inhibition in paw volume by co-  
 463 crystal formulation as compared to standard drug in wistar rats whereas *in-vivo* analgesic activity  
 464 further showed that pain threshold has significantly enhanced. The half maximal inhibitory  
 465 concentration (IC<sub>50</sub>) values for *in-vitro* anti-inflammatory activity exhibited almost 8-fold  
 466 amplification in activity indicating higher anti-inflammatory effect of optimized co-crystal batch  
 467 as compared to pure drug ketoprofen. On that account, it can be concluded that co-crystallization  
 468 proves to be a promising technique for enhancing the solubility characteristics of BCS -II drugs.

## 469 CONFLICT OF INTEREST

470 The authors report no conflicts of interest.

## 471 Statement of Animal Rights

472 The procedure followed for animal handling is in accordance with the protocol as approved for  
473 animal study (CPCSEA Reg. no-IAEC/2020/10-18) by the Institutional Animal Ethical  
474 Committee, Guru Jambheshwar University of Science and Technology, Hisar, India.

475

476

477 **REFERENCES**

- 478 1. Sarraguça, M. C., Ribeiro, P. R., Dos Santos, A. O., & Lopes, J. A. (2015). Batch  
479 statistical process monitoring approach to a cocrystallization process. *Journal of*  
480 *pharmaceutical sciences*, 104(12), 4099-4108, <https://doi.org/10.1002/jps.24623>.
- 481 2. Soares, F. L., & Carneiro, R. L. (2013). Green synthesis of ibuprofen–nicotinamide  
482 cocrystals and in-line evaluation by Raman spectroscopy. *Crystal growth &*  
483 *design*, 13(4), 1510-1517., <https://doi.org/10.1021/cg3017112>.
- 484 3. Harriss, B. I., Vella-Zarb, L., Wilson, C., & Evans, I. R. (2014). Furosemide cocrystals:  
485 Structures, hydrogen bonding, and implications for properties. *Crystal growth &*  
486 *design*, 14(2), 783-791, <https://doi.org/10.1021/cg401662d>.
- 487 4. Padrela, L., Rodrigues, M. A., Velaga, S. P., Matos, H. A., & de Azevedo, E. G. (2009).  
488 Formation of indomethacin–saccharin cocrystals using supercritical fluid  
489 technology. *European Journal of Pharmaceutical Sciences*, 38(1), 9-17,  
490 <https://doi.org/10.1016/j.ejps.2009.05.010>.
- 491 5. Chow, S. F., Shi, L., Ng, W. W., Leung, K. H. Y., Nagapudi, K., Sun, C. C., & Chow, A.  
492 H. (2014). Kinetic entrapment of a hidden curcumin cocrystal with  
493 phloroglucinol. *Crystal growth & design*, 14(10), 5079-5089,  
494 <https://doi.org/10.1021/cg5007007>.
- 495 6. Childs, S. L., Stahly, G. P., & Park, A. (2007). The salt– cocrystal continuum: the  
496 influence of crystal structure on ionization state. *Molecular pharmaceuticals*, 4(3), 323-  
497 338,  
498 <https://doi.org/10.1021/mp0601345>.
- 499 7. Berry, D. J., & Steed, J. W. (2017). Pharmaceutical cocrystals, salts and multicomponent  
500 systems; intermolecular interactions and property based design. *Advanced drug delivery*  
501 *reviews*, 117, 3-24, <https://doi.org/10.1016/j.addr.2017.03.003>.
- 502 8. da Silva, C. C., Pepino, R. D. O., de Melo, C. C., Tenorio, J. C., & Ellena, J. (2014).  
503 Controlled Synthesis of New 5-Fluorocytosine Cocrystals Based on the p K a  
504 Rule. *Crystal Growth & Design*, 14(9), 4383-4393, <https://doi.org/10.1021/cg500502j>.
- 505 9. Aitipamula, S., Chow, P. S., & Tan, R. B. (2014). Polymorphism in cocrystals: a review  
506 and assessment of its significance. *CrystEngComm*, 16(17), 3451-3465,  
507 <https://doi.org/10.1039/C3CE42008F>.

- 508 10. Lee, K. S., Kim, K. J., & Ulrich, J. (2015). Formation of Salicylic Acid/4, 4'-Dipyridyl  
509 Cocrystals Based on the Ternary Phase Diagram. *Chemical Engineering &*  
510 *Technology*, 38(6), 1073-1080, <https://doi.org/10.1002/ceat.201400738>
- 511 11. Shayanfar, A., & Jouyban, A. (2014). Physicochemical characterization of a new  
512 cocrystal of ketoconazole. *Powder technology*, 262, 242-248,  
513 <https://doi.org/10.1016/j.powtec.2014.04.072>.
- 514 12. Ganesh, M., Ubaidulla, U., Rathnam, G., & Jang, H. T. (2019). Chitosan-telmisartan  
515 polymeric cocrystals for improving oral absorption: In vitro and in vivo  
516 evaluation. *International journal of biological macromolecules*, 131, 879-885,  
517 <https://doi.org/10.1016/j.ijbiomac.2019.03.141>.
- 518 13. Mutalik, S., Anju, P., Manoj, K., & Usha, A. N. (2008). Enhancement of dissolution rate  
519 and bioavailability of aceclofenac: a chitosan-based solvent change  
520 approach. *International journal of pharmaceutics*, 350(1-2), 279-290,  
521 <https://doi.org/10.1016/j.ijpharm.2007.09.006>.
- 522 14. Alvani, A., Jouyban, A., & Shayanfar, A. (2019). The effect of surfactant and polymer on  
523 solution stability and solubility of tadalafil-methylparaben cocrystal. *Journal of*  
524 *Molecular Liquids*, 281, 86-92, <https://doi.org/10.1016/j.molliq.2019.02.080>.
- 525 15. Rahman, Z., Agarabi, C., Zidan, A. S., Khan, S. R., & Khan, M. A. (2011). Physico-  
526 mechanical and stability evaluation of carbamazepine cocrystal with nicotinamide. *Aaps*  
527 *Pharmscitech*, 12(2), 693-704, <https://doi.org/10.1208/s12249-011-9603-4>.
- 528 16. Lyn, L. Y., Sze, H. W., Rajendran, A., Adinarayana, G., Dua, K., & Garg, S. (2011).  
529 Crystal modifications and dissolution rate of piroxicam. *Acta Pharmaceutica*, 61(4), 391-  
530 402, <https://doi.org/10.2478/v10007-011-0037-z>.
- 531 17. Zhang, Y. X., Wang, L. Y., Dai, J. K., Liu, F., Li, Y. T., Wu, Z. Y., & Yan, C. W.  
532 (2019). The comparative study of cocrystal/salt in simultaneously improving solubility  
533 and permeability of acetazolamide. *Journal of Molecular Structure*, 1184, 225-232,  
534 <https://doi.org/10.1016/j.molstruc.2019.01.090>.
- 535 18. Gautam, M. K., Besan, M., Pandit, D., Mandal, S., & Chadha, R. (2019). Cocrystal of 5-  
536 fluorouracil: Characterization and evaluation of biopharmaceutical parameters. *AAPS*  
537 *PharmSciTech*, 20(4), 149, <https://doi.org/10.1208/s12249-019-1360-9>.

- 538 19. Kaleemullah M., Jiyauddin K., Thiban E., Raska S., AL-dhalli S., Budiasih S., Gamal O.E.,  
539 Fadli A., & Eddy Y. Development and evaluation of ketoprofen sustained release matrix  
540 tablet using Hibiscus rosa- sinensis leaves mucilage. *Saudi pharmaceutical Journal* 25(5):  
541 770-779, <https://doi.org/10.1016/j.jsps.2016.10.006>.
- 542 20. Bhatia, M., & Devi, S. Development, Characterisation and Evaluation of PVP K-30/PEG  
543 Solid Dispersion Containing Ketoprofen. *ACTA Pharmaceutica Scientia*, 58(1),  
544 DOI: 10.23893/1307-2080.APS.05806.
- 545 21. Bhatia, M., & Devi, R. (2019). Enhanced Solubility and Drug Release of Ketoprofen  
546 Using Lyophilized Bovine Serum Albumin Solid Dispersion. *ACTA Pharmaceutica*  
547 *Scientia*, 57(1), DOI: 10.23893/1307-2080.APS.05703.
- 548 22. Vittal, G. V., Deveswaran, R., Bharath, S., Basavaraj, B. V., & Madhavan, V. (2012).  
549 Formulation and characterization of ketoprofen liquid compact by Box-Behnken  
550 design. *International journal of pharmaceutical investigation*, 2(3), 150,  
551 doi: [10.4103/2230-973X.104398](https://doi.org/10.4103/2230-973X.104398).
- 552 23. Nikumbh, K. V., Sevankar, S. G., & Patil, M. P. (2015). Formulation development, in  
553 vitro and in vivo evaluation of microemulsion-based gel loaded with ketoprofen. *Drug*  
554 *delivery*, 22(4), 509-515, <https://doi.org/10.3109/10717544.2013.859186>.
- 555 24. Ambala, R., & Vemula, S. K. (2015). Formulation and characterization of ketoprofen  
556 emulgels. *Journal of Applied Pharmaceutical Science*, 5(7), 112-117, DOI:  
557 10.7324/JAPS.2015.50717.
- 558 25. Attia, M. F., Anton, N., Khan, I. U., Serra, C. A., Messaddeq, N., Jakhmola, A., &  
559 Vandamme, T. (2016). One-step synthesis of iron oxide polypyrrole nanoparticles  
560 encapsulating ketoprofen as model of hydrophobic drug. *International Journal of*  
561 *Pharmaceutics*, 508(1-2), 61-70, <https://doi.org/10.1016/j.ijpharm.2016.04.073>.
- 562 26. Shah, P. P., Desai, P. R., & Singh, M. (2012). Effect of oleic acid modified polymeric  
563 bilayered nanoparticles on percutaneous delivery of spantide II and ketoprofen. *Journal*  
564 *of controlled release*, 158(2), 336-345, <https://doi.org/10.1016/j.jconrel.2011.11.016>.
- 565 27. Gul, R., Ahmed, N., Ullah, N., Khan, M. I., & Elaissari, A. (2018). Biodegradable  
566 ingredient-based emulgel loaded with ketoprofen nanoparticles. *AAPS*  
567 *PharmSciTech*, 19(4), 1869-1881, <https://doi.org/10.1208/s12249-018-0997-0>.

- 568 28. Kheradmandnia, S., Vasheghani-Farahani, E., Nosrati, M., & Atyabi, F. (2010).  
569 Preparation and characterization of ketoprofen-loaded solid lipid nanoparticles made  
570 from beeswax and carnauba wax. *Nanomedicine: Nanotechnology, Biology and*  
571 *Medicine*, 6(6), 753-759, <https://doi.org/10.1016/j.nano.2010.06.003>.
- 572 29. Xi, M. M., Wang, X. Y., Fang, K. Q., & Gu, Y. (2005). Study on the characteristics of  
573 pectin–ketoprofen for colon targeting in rats. *International journal of*  
574 *pharmaceutics*, 298(1), 91-97, <https://doi.org/10.1016/j.ijpharm.2005.04.012>.
- 575 30. Kluge, J., Fusaro, F., Mazzotti, M., & Muhrer, G. (2009). Production of PLGA micro-  
576 and nanocomposites by supercritical fluid extraction of emulsions: II. Encapsulation of  
577 Ketoprofen. *The Journal of Supercritical Fluids*, 50(3), 336-343,  
578 <https://doi.org/10.1016/j.supflu.2009.05.002>.
- 579 31. Perpétuo, G. L., Chierice, G. O., Ferreira, L. T., Fraga-Silva, T. F. C., Venturini, J.,  
580 Arruda, M. S. P., & Castro, R. A. E. (2017). A combined approach using differential  
581 scanning calorimetry with polarized light thermomicroscopy in the investigation of  
582 ketoprofen and nicotinamide cocrystal. *Thermochimica Acta*, 651, 1-10,  
583 <https://doi.org/10.1016/j.tca.2017.02.014>.
- 584 32. Sanphui, P., Kumar, S. S., & Nangia, A. (2012). Pharmaceutical cocrystals of  
585 niclosamide. *Crystal growth & design*, 12(9), 4588-4599,  
586 <https://doi.org/10.1021/cg300784v>.
- 587 33. Bhogala, B. R., Basavoju, S., & Nangia, A. (2005). Tape and layer structures in  
588 cocrystals of some di- and tricarboxylic acids with 4, 4'-bipyridines and isonicotinamide.  
589 From binary to ternary cocrystals. *Cryst Eng Comm*, 7(90), 551-562,  
590 <https://doi.org/10.1039/B509162D>.
- 591 34. Sarkar, A., & Rohani, S. (2015). Cocrystals of acyclovir with promising physicochemical  
592 properties. *Journal of pharmaceutical sciences*, 104(1), 98-105,  
593 <https://doi.org/10.1002/jps.24248>
- 594 35. Farrag, Y., Ide, W., Montero, B., Rico, M., Rodríguez-Llamazares, S., Barral, L., &  
595 Bouza, R. (2018). Preparation of starch nanoparticles loaded with quercetin using  
596 nanoprecipitation technique. *International journal of biological macromolecules*, 114,  
597 426-433, <https://doi.org/10.1016/j.ijbiomac.2018.03.134>.

- 598 36. Luo, Y., Chen, S., Zhou, J., Chen, J., Tian, L., Gao, W., & Zhou, Z. (2019). Luteolin  
599 cocrystals: Characterization, evaluation of solubility, oral bioavailability and theoretical  
600 calculation. *Journal of Drug Delivery Science and Technology*, 50, 248-254,  
601 <https://doi.org/10.1016/j.jddst.2019.02.004>.
- 602 37. Chavan, R. R., & Hosamani, K. M. (2018). Microwave-assisted synthesis, computational  
603 studies and antibacterial/anti-inflammatory activities of compounds based on coumarin-  
604 pyrazole hybrid. *Royal Society open science*, 5(5), 172435,  
605 <https://doi.org/10.1098/rsos.172435>.
- 606 38. Alshaikh, R. A., Essa, E. A., & El Maghraby, G. M. (2019). Eutexia for enhanced  
607 dissolution rate and anti-inflammatory activity of nonsteroidal anti-inflammatory agents:  
608 Caffeine as a melting point modulator. *International journal of pharmaceutics*, 563, 395-  
609 405, <https://doi.org/10.1016/j.ijpharm.2019.04.024>.
- 610 39. Komakech, R., Kim, Y. G., Matsabisa, G. M., & Kang, Y. (2019). Anti-inflammatory and  
611 analgesic potential of Tamarindus indica Linn.(Fabaceae): a narrative review. *Integrative  
612 Medicine Research*, 8(3), 181-186, <https://doi.org/10.1016/j.imr.2019.07.002>
- 613 40. Mondal, A., Maity, T. K., & Bishayee, A. (2019). Analgesic and Anti-Inflammatory  
614 Activities of Quercetin-3-methoxy-4'-glucosyl-7-glucoside Isolated from Indian  
615 Medicinal Plant Melothria heterophylla. *Medicines*, 6(2), 59,  
616 <https://doi.org/10.3390/medicines6020059>.
- 617 41. Khullar, R., Kumar, D., Seth, N., & Saini, S. (2012). Formulation and evaluation of  
618 mefenamic acid emulgel for topical delivery. *Saudi pharmaceutical journal*, 20(1), 63-67,  
619 <https://doi.org/10.1016/j.jsps.2011.08.001>.
- 620 42. Kulkarni, S. K. (1980). Heat and other physiological stress-induced analgesia:  
621 catecholamine mediated and naloxone reversible response. *Life sciences*, 27(3), 185-188,  
622 [https://doi.org/10.1016/0024-3205\(80\)90136-8](https://doi.org/10.1016/0024-3205(80)90136-8).
- 623 43. Sun, S., Zhang, X., Cui, J., & Liang, S. (2020). Identification of the Miller indices of a  
624 crystallographic plane: a tutorial and a comprehensive review on fundamental theory,  
625 universal methods based on different case studies and matters needing  
626 attention. *Nanoscale*, 12(32), 16657-16677, <https://doi.org/10.1039/D0NR03637D>.
- 627 44. Yadav, A. V., Shete, A. S., Dabke, A. P., Kulkarni, P. V., & Sakhare, S. S. (2009). Co-  
628 crystal: a novel approach to modify physicochemical properties of active pharmaceutical

629 ingredients. *Indian journal of pharmaceutical sciences*, 71(4), 359, [10.4103/0250-](https://doi.org/10.4103/0250-474X.57283)  
630 [474X.57283](https://doi.org/10.4103/0250-474X.57283).

631 45. Stewart, J. J. P. (2016). Stewart Computational Chemistry, MOPAC2016. *Colorado*  
632 *Springs*. Available online at: <http://OpenMOPAC.net>.

633 46. Alex A. Granovsky, Firefly version 8, www,  
634 <http://classic.chem.msu.su/gran/firefly/index.html>

635 47. Tian Lu, Feiwu Chen, *J. Comput. Chem.*, 33, 580-592 (2012).

636 48. Humphrey, W., Dalke, A., & Schulten, K. (1996). VMD-Visual Molecular Dynamics, *J*  
637 *Molec Graphics*.

638

639

640

641

642

643

644

645

646

647

648